The upgraded performance of CAST

Jaime Ruz Armendáriz. University of Zaragoza

On behalf of the CAST collaboration
DESY (Hamburg), 18th of June 2008

The CAST Experiment

Principle of detection

Production of axions: Primakoff effect of thermal photons in the Solar core.

$$\frac{d\phi_a}{dE_a} = 6.020 \times 10^{10} \cdot g_{10}^2 \cdot E_a^{2.481} e^{-E_a/1.205}\ \mathrm{cm}^{-2}\mathrm{s}^{-1}\mathrm{keV}^{-1} \quad (1)$$

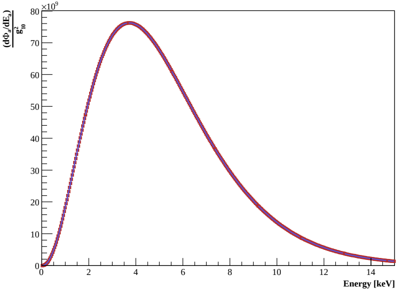

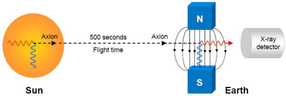

Detection principle: axions converting to photons in a magnetic field.

$$\mathcal{N}_\gamma = \int_0^L \frac{d\phi_a}{dE_a}(E_a) \cdot \mathcal{P}_{a\rightarrow\gamma}(E_a) \cdot S \cdot t \cdot \varepsilon(E_a) \cdot dE_a \quad (2)$$

Coherence of conversion

Conversion Probability

$$\mathcal{P}_{a\rightarrow\gamma} = \left[\frac{g_{a\gamma\gamma}}{10^{-10}\,GeV^{-1}}\right]^2 \left[\frac{B_\perp}{2}\right]^2 \cdot \frac{1}{q^2+\Gamma^2/4} \cdot \left[1+e^{-\Gamma L} - 2e^{-\Gamma L/2}\cos qL\right] \qquad (3)$$

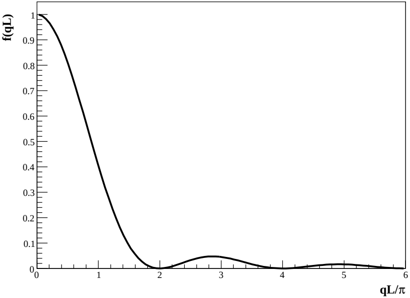

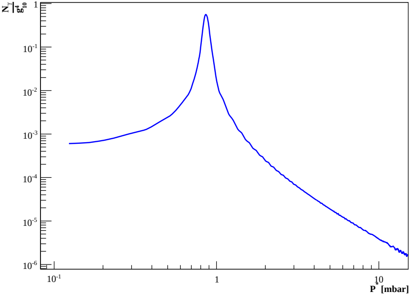

Coherence Condition

$$|m_a^2 - m_\gamma^2| \ll 2\frac{E_a}{L} \qquad (4)$$

Damping Gas

Absorption of converted photons in Helium

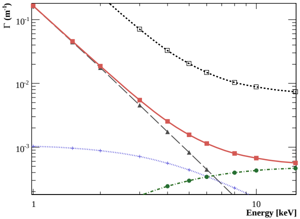

- Photoelectric effect
- Coherent Scattering (Rayleigh)
- Incoherent Scattering (Compton)

Absorption is Pressure and Energy dependent

$$\log_{10}\Gamma_{P_{He},E_a} = -2.0282\cdot\log_{10}^{5}E_a + 4.7254\cdot\log_{10}^{4}E_a - 2.3282\cdot\log_{10}^{3}E_a + $$
$$+ 0.4296\cdot\log_{10}^{2}E_a - 3.1864\cdot\log_{10}E_a - 0.7834 + log_{10}P_{He} \tag{5}$$

General description

- *Decommissioned prototype LHC dipole magnet*
- *Superconducting: operation at* 1.8 K
- *Magnetic field intensity:* 8.97 T
- *Magnet length: 9.26 m*
- *Exposure area: Four ports of* 43 mm *diameter*

Rotating platform
(Vertical: ±8°, Horizontal: ±40°)
∼ 90 min per port and day
3 X-ray detectors
X-ray focusing device

CAST Physics program

- ***CAST Phase I***
  - *Vacuum operation. Completed during* ***2003*** *and* ***2004***
- ***CAST Phase II***
  - ^{4}*He run. Completed during* ***2005*** *and* ***2006***
    - ^{4}***He vapor pressure at*** 16.4 mbar
    - ***Mass range covered up to*** 13.4 mbar

$$0.2\,\mathrm{eV} < m_a < 0.39\,\mathrm{eV} \tag{6}$$

  - ^{3}*He run. Started in* ***2007*** *...*
    - ^{3}***He vapor pressure at*** 135.6 mbar
    - ***Mass range to be covered up to*** 120 mbar

$$0.39\,\mathrm{eV} < m_a < 1.20\,\mathrm{eV} \tag{7}$$

- ***CAST at present***

$$0.39\,\mathrm{eV} < m_a < 0.48\,\mathrm{eV} \quad \textbf{Completed!!} \tag{8}$$

READY FOR KSVZ MODELS !!

- ***Low energy axions (See Prof. Cantatore)***

CAST Vacuum Result

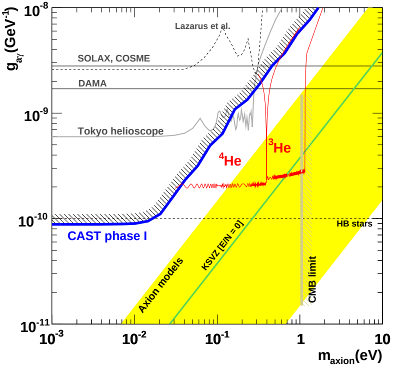

Exclusion plot for the axion-to-photon coupling relative to its mass.
CAST Phase I

$$g_{a\gamma\gamma} \lesssim 8.8 \times 10^{-11}\ \mathrm{GeV}^{-1}\ (95\,\%\ \mathrm{C.L})\quad \mathrm{m_a} < 0.02\,\mathrm{eV} \tag{9}$$

CAST ^{4}He Result

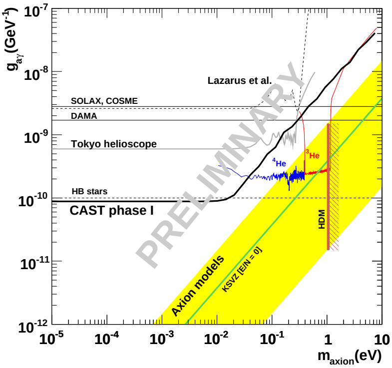

Exclusion plot for the axion-to-photon coupling relative to its mass.
CAST ^{4}He *Phase*

$$g_{a\gamma\gamma} \lesssim 2.22 \times 10^{-10}\,\mathrm{GeV}^{-1}\ (95\,\%\,\mathrm{C.L})\ \ \mathrm{m_a} < 0.39\,\mathrm{eV} \qquad (10)$$

CAST Combined Result

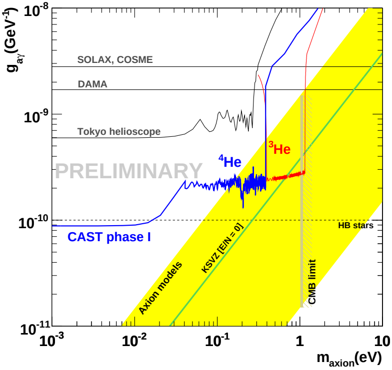

Exclusion plot for the axion-to-photon coupling relative to its mass.
CAST Phases I and $^{4}\mathrm{He}$

The CAST Upgrade

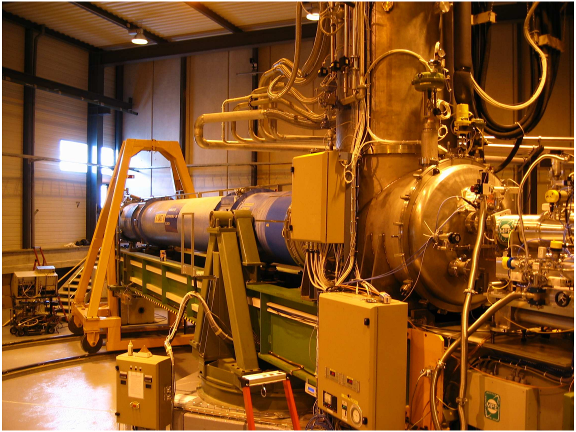

Gas System Requirements

Gas Confinement

- *X-ray Windows*
  - *High X-ray transmission*
    - 15 μm *polypropylene*
    - *Transmission is* $\sim$ 95 % @ 4.2 keV
  - *Robust (Strong-back)*
    - $\forall 5.2$ mm, $|0.3$ mm, $\square 5$ mm
  - *Hermeticity tested* $< 1 \times 10^{-7}$ mbar l s^{-1}
  - *Pressure Tested*
    - *All cycled at* 1 bar
    - *Prototype holds* 3.5 bar
  - *Regularly baked-out to avoid cryopumping*

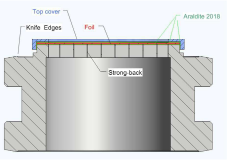

Window design

Cold Window

Gas System Requirements

Gas Injection

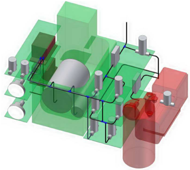

Metering modeling

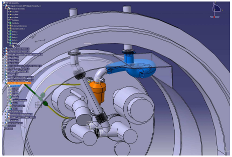

MFB modeling

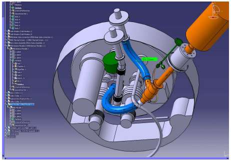

MRB modeling

- *Metrological Pressure Measurement*
  - *Stability, Accuracy, Reproducibility* ($\lesssim 0.01\,\mathrm{mbar}$)
  - *Thermally controlled calibrated volumes*
  - *Homogeneous thermalization with superfluid Helium*
  - *Accuracy of the gas measurements better than 60 ppm*
  - *Possibiliy of Helium purification in case of leaks*
  - *Recovery line to avoid the sudden increase of pressure during a QUENCH* ($\sim 20\,\mathrm{bar}$)

Design

Metering stage and purification system

Metering device

Cold Trap

Computational Fluid Dynamics Modeling

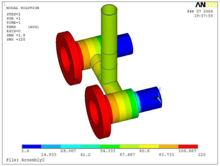

Simulation

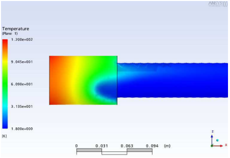

Simulation

Design

Instalation of the gas system

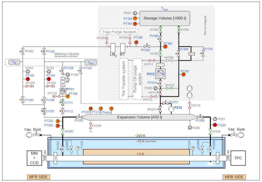

Gas system Schematics

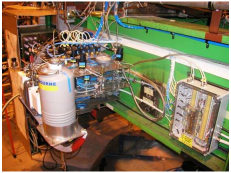

Metering Volume

Instalation of the Expansion Volume and Recovery System

Expansion Volume

Recovery System

Reliability

ThermoAcoustic Oscillations

"Expontaneous acoustic oscillations of gas columns can be generated in a tube with step temperature gradients without external force."

Agreement with literature. Full Control of TAO's

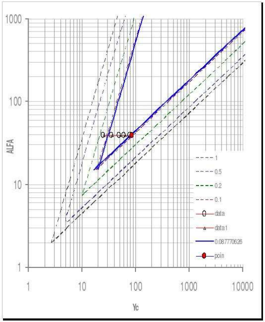

Open Valves at 80 K

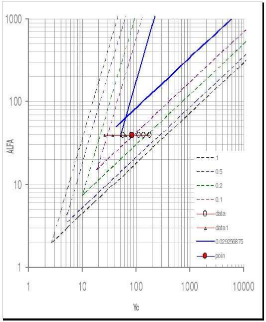

Needle valves closed at 80 K

The CAST Detectors

Exhaustive revision and upgrade of the CAST detectors

- ***The CCD Detector together with an X-ray focusing device***
  - *VT4 port.*
- ***Sunsise Micromegas***
  - *Bulk technology (VT3 port).*
- ***Sunset Micromegas***
  - *Replacement of the TPC detector (VT1 and VT2 ports).*
  - *MicroBulk technology (VT1 port).*
  - *Bulk technology (VT2 port).*
- ***The visible detector (See Prof. Cantatore)***

The X-ray telescope

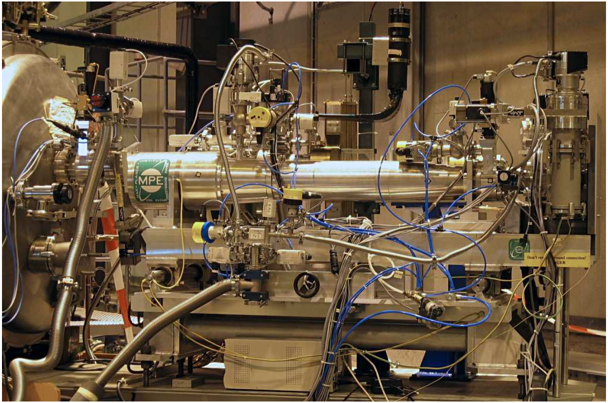

The CCD detector

Replacement of the pn-CCD detector

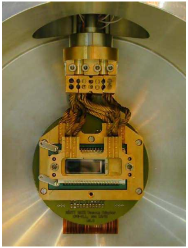

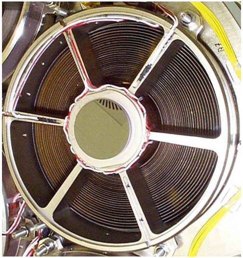

- *Spare pn-CCD chip of the same type has been characterized and installed in order to avoid noisy pixels and saturation problems*
- *New calibrator design and installation*
- *The X-ray telescope has been tested at the PANTER X-ray facility. Any loss of efficiency due to potential surface contamination has been excluded*

The Micromegas detectors

- **Sunrise side:**
  - Bulk MM Installation.
  - New line was installed with possibility to use an X-Ray focusing device.
  - Shielding of the detector.
- **Sunset side:**
  - In June 2007 the replacement of the TPC detector was approved.
  - The Bulk/Microbulk Micromegas detectors were chosen.
  - Shielding of the detectors.

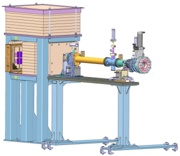

New Sunrise Line

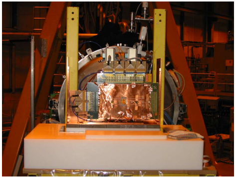

TPC detector of the CAST experiment

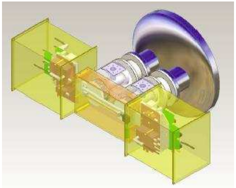

New sunset micromegas design

The Sunrise micromegas

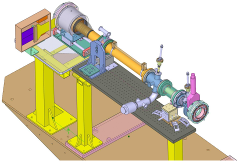

Line design of the Sunrise Micromega

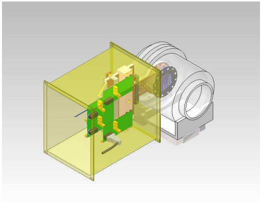

Shielding design of the Sunrise Micromega

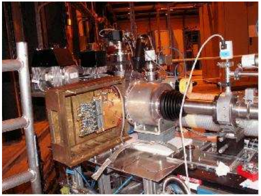

Front view of the Sunrise micromega inner shielding

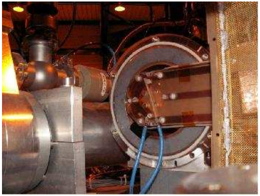

Back view of the Sunrise Micromega before closing the inner shielding

The Sunset micromegas

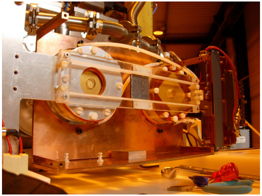

Installation of the Sunset Micromegas

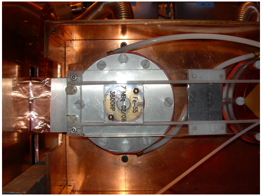

Calibrator of the Sunset Micromegas

Installation of the shielding for the Sunset Micromegas

Present view of the Sunset Micromegas

The Behaviour of the detectors

Very Preliminary Numbers

$$\textit{CCD Background (2008)} = 8.76 \times 10^{-5}\,\mathrm{counts\,keV^{-1}cm^{-2}sec^{-1}} \qquad (11)$$
$$\textbf{Expected (2008)} \sim 0.15\,\mathrm{counts/setting}$$

$$\textit{Sunrise Bulk Background} = 7.66 \times 10^{-7}\,\mathrm{counts\,keV^{-1}cm^{-2}sec^{-1}} \qquad (12)$$
$$\textbf{Expected (2008)} \sim 0.16\,\mathrm{counts/setting}$$

$$\textit{Sunset Bulk Background} = 8.89 \times 10^{-6}\,\mathrm{counts\,keV^{-1}cm^{-2}sec^{-1}} \qquad (13)$$
$$\textbf{Expected (2008)} \sim 1.75\,\mathrm{counts/setting}$$

$$\textit{Sunset MicroBulk Background} = 1.99 \times 10^{-5}\,\mathrm{counts\,keV^{-1}cm^{-2}sec^{-1}} \qquad (14)$$
$$\textbf{Expected (2008)} \sim 4\,\mathrm{counts/setting}$$

The Behaviour of the detectors

$$\begin{aligned} \textit{TPC Background} &= 4.59 \times 10^{-5}\,\mathrm{counts\,keV^{-1}cm^{-2}sec^{-1}} \\ \textbf{Expected (2006)} &\sim 50\,\mathrm{counts/setting} \end{aligned} \quad (15)$$

$$\begin{aligned} \textit{V5 Micromegas Background} &= 4.62 \times 10^{-5}\,\mathrm{counts\,keV^{-1}cm^{-2}sec^{-1}} \\ \textbf{Expected (2006)} &\sim 28\,\mathrm{counts/setting} \end{aligned} \quad (16)$$

New CCD detector is working as well as its predeccessor

Background level of TPC has been improved by a factor ~ 20

Sunrise micromegas background level is really promissing

The axion Searches

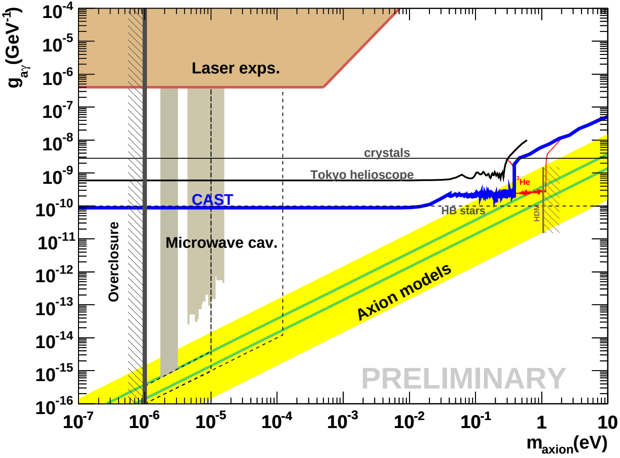

CAST experiment in the different axion searches

Appendix

A. ***The Micromegas detectors***
B. ***ThermoAcoustic Oscillations***
C. ***Gravity Role***

The Micromegas detectors

- **Conventional Micromegas:** The pillars are attached to the mesh. A supporting ring is adjusting the mesh on top of the readout plane and the High Voltage fixes the mesh to the read out plane.
- **Bulk Micromegas:** The pillars are attached to a woven mesh (30 μm Stainless Steel) and to the readout plane. Reachable Energy resolution (18 % @ 5.9 keV)
  - *Advantages:* Uniformity, easy use, robust.
  - *Disadvantages:* Limited Energy Resolution due to mess thickness.

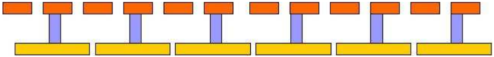

Bulk schematics. $\sim$ **128** μm ***gap between mesh and the readout plane***

- **MicroBulk Micromegas:**The pillars are constructed by chemical process of a kapton foil, that is attached to the mesh (5 μm Cu) and to the readout plane. Reachable Energy resolution (better than 15 % @ 5.9 keV)
  - *Advantages:*Uniformity, Energy resolution and better stability at long term runs.
  - *Disadvantages:* Complexity in manufacturing process, fragility.

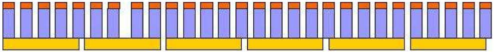

MicroBulk schematics. $\sim$ **50** μm ***gap between mesh and the readout plane***

Reliability

ThermoAcoustic Oscillations

"Expontaneous acoustic oscillations of gas columns can be generated in a tube with step temperature gradients without external force."

How to stop them?

- *During ^{4}He Phase*
  - *Pressure Transducers inside the cold bore*
  - *Home made dampers to "block" the flow.*
  - *Fast Monitoring*
  - ***Oscillations Stoped***

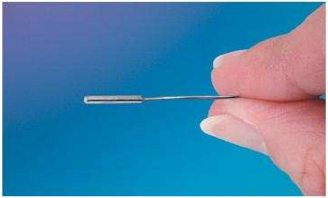

Transducer

Reliability

- *Implemented for ^{3}He Phase*
  - *Dampers to "block" the flow are ineffective due to the high pressures.*
  - *Cryogenics needle valves to block the flow and open in case of QUENCH*
  - ***Oscillations Stoped***

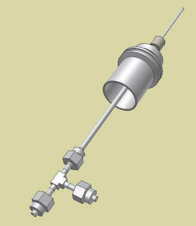

Needle valve design

Needle valve

Needle installation

Reliability

Agreement with literature. Full Control of TAO's

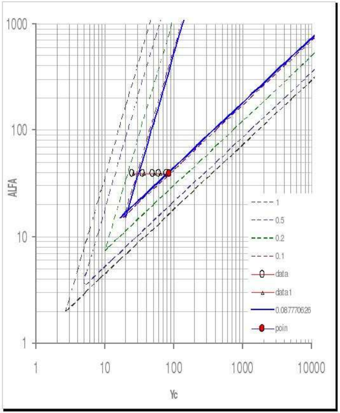

Open Valves at **80** K

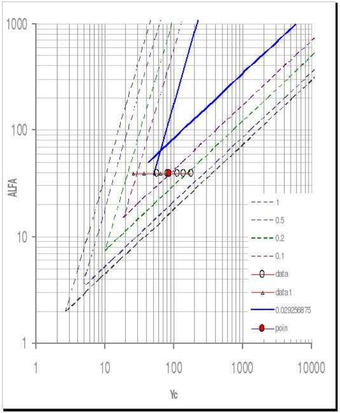

Needle valves closed at **80** K

Gravity role

$$A(L)|a(0)\rangle_{BMMR} = \frac{g_{a\gamma\gamma}}{2} B\, e^{-\int_o^L dz' \Gamma/2} \times \int_0^L dz'\, e^{i \int_0^{z'} dz'' \left(\frac{m_\gamma^2(z'')-m_a^2}{2E_a}\frac{1}{\hbar c} - i\Gamma/2\right)} \quad (17)$$

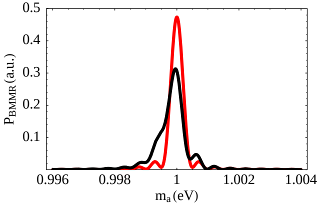

$$n_e(z) = n_e^o\left[1 - \frac{(2z - L) M_{He}\, g\, \sin\theta}{2kT}\right] \quad (18)$$

Reduction from 0.47 to 0.31 (arbitrary units)

Probability of the axion-to-photon conversion P_{BMMR}
Calculated for an effective photon mass of 1 eV
Tilt angles of 0^o (red line) and 8^0 (black line)

Thanks Biljana and Milica

Gravity role

$$\langle A(L)|a(0)\rangle_{CNA} = \frac{-i\,g_{a\gamma\gamma}}{2} B\, e^{i\int_o^L dz' \left(\frac{m_\gamma^2(z')-m_a^2}{2E_a}\frac{1}{\hbar c}+i\Gamma/2\right)} \times \int_0^L dz'\, e^{i\int_0^{z'} dz'' \left(\frac{m_\gamma^2(z'')-m_a^2}{2E_a}\frac{1}{\hbar c}-i\Gamma/2\right)} \quad (19)$$

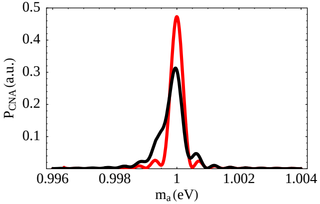

$$\frac{m_\gamma(z)}{1\,\mathrm{eV}} \simeq 3.716 \times 10^{-11}\sqrt{\frac{n_e(z)}{1\,\mathrm{cm}^3}} \quad (20)$$

Reduction from 0.47 to 0.31 (arbitrary units)

Probability of the axion-to-photon conversion P_{CNA}
Calculated for an effective photon mass of 1 eV
Tilt angles of 0^o (red line) and 8^0 (black line)

Thanks Biljana and Milica

Gravity role

$$R_{CNA} = e^{-\Gamma} \frac{\pi}{2b} \left| e^{ia^2/2b} \left[erf\left[\sqrt{\frac{i}{2b}}(a+b) \right] - erf\left[\sqrt{\frac{i}{2b}} a \right] \right] \right| \tag{21}$$

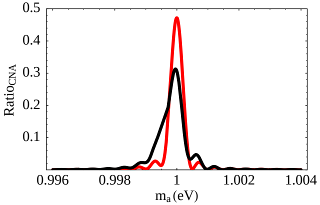

Reduction from 0.47 to 0.26 (arbitrary units)

Ratio CNA as a function of the axion mass
Calculated for an effective photon mass of 1 eV
Tilt angles of 0^{o} ***(red line) and*** 8^{0} ***(black line)***

Thanks Biljana and Milica

Gravity role

$$R_{CNA} = e^{-\Gamma} \frac{\pi}{2b} \left| e^{ia^2/2b} \left[erf\left[\sqrt{\frac{i}{2b}}(a+b) \right] - erf\left[\sqrt{\frac{i}{2b}} a \right] \right] \right| \quad (22)$$

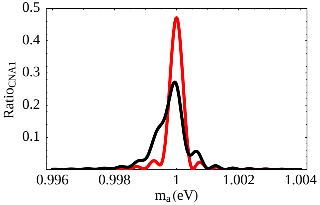

Reduction from 0.47 to 0.26 (arbitrary units)

Ratio CNA_1 as a function of the axion mass
Calculated for an effective photon mass of 1 eV
Tilt angles of 0^o (red line) and 8^0 (black line)

Thanks Biljana and Milica